Electronic Supplementary Material (ESI) for Journal of Materials Chemistry A.

Identification of Optimal Active Boron Site for N_2 Reduction

Hui Yin[1], Li-Yong Gan[1,2]*, and Ping Wang[1]*

[1]School of Materials Science and Engineering, Key Laboratory of Advanced Energy Storage Materials of Guangdong Province, South China University of Technology, Guangzhou, 510641, P.R. China

[2]Institute for Structure and Function and Department of Physics, Chongqing University, Chongqing, 400030, China

*E-mail: ganly@cqu.edu.cn (L.-Y. Gan) and mspwang@scut.edu.cn (P. Wang).

*Tel: +86 20 3938 0583.

Free Energy Calculations

The associated free energy change (ΔG) of each step was determined according to a computational hydrogen electrode model proposed by Nørskov et al.,[1] and is calculated by taking gas-phase N_2 and H_2 as reference states

$$\Delta G = \Delta E + \Delta ZPE - T\Delta S + \Delta G_U + \Delta G_{pH}$$

where ΔE, ΔZPE, and ΔS represent the reaction energy, zero point energy difference and entropy change of each step, respectively. The temperature (T) is set to be 298.15 K. ΔG_U is the effect of an operating bias U, and equals $-neU$ with n being the number of electrons involved in the reaction. ΔG_{pH} is the correction of the H^+ concentration in electrolytes, and was calculated as $\Delta G_{pH} = 0.059 \times pH$. Since the overpotential remains the same with increasing pH value, pH was assumed to be zero.

The entropies and zero-point energy were calculated based on the vibrational frequencies. The entropy is calculated as

$$S(T) = \sum_{i=1}^{3N} [- R\ln\left(1 - e^{-\frac{h\nu_i}{k_B T}}\right) + \frac{N_A h\nu_i \, e^{-h\nu_i / k_B T}}{T \left(1 - e^{-h\nu_i / k_B T}\right)}]$$

in which R, h, k_B, N_A, ν_i, N and T is the universal gas constant, Planck's constant, Boltzmann's constant, Avogadro's number, frequency of the normal mode, number of adsorbed atoms and temperature (298.15 K), respectively. Entropies of the gas-phase N_2 and H_2 were taken from the NIST database. The zero point energy is defined as

$$E_{ZPE} = \frac{1}{2} \sum_{i=1}^{N_{modes}} h\nu_i$$

where N_{modes} is the number of vibrational modes. Then, ΔE_{ZPE} and ΔS are the differences in zero point energy and entropy, respectively, between the adsorbed species and gas-phase molecules. The operating bias U_L is the applied potential required to eliminate the energy barrier of the potential-limiting step and is calculated as $-\Delta G_{pls}/e$, where ΔG_{pls} is the free energy difference of the potential-limiting step according to the standard hydrogen electrode (SHE).[2]

The decomposition of N-doped substrate to release NH_3 can be expressed as:

$$B/C_2N - s + 3(H^+ + e^-) \rightarrow B/C_2N - s' + NH_3(g)$$

where B/C_2N-s' is the structure of B/C_2N-s after losing one nitrogen atom. Hence, the required potential (U_d vs. SHE) to form NH_3 by the decomposition of catalysts can be expressed as:
$U_d = \Delta G_d/3e$

Table S1. The free energies of each step via alternating and distal mechanisms on B/C_2N-a and B/C_2N-s in a 2 × 2 supercell and those on B/C_2N-s in a 1 × 1 supercell.

Distal mechanism			Alternating mechanism			
species	ΔG (eV) B/C_2N-a (2 × 2)	ΔG (eV) B/C_2N-s (2 × 2)	species	ΔG (eV) B/C_2N-a (2 × 2)	ΔG (eV) B/C_2N-s (2 × 2)	ΔG (eV) B/C_2N-s (1 × 1)
N_2	0	0	N_2	0	0	0
$*N_2H$	-0.77	-0.37	$*N_2H$	-0.77	-0.37	-0.58
$*NNH_2$	-1.41	-0.77	*NHNH	-1.69	-0.57	-0.86
$*NNH_3$	-1.43	-0.48	$*NH_2NH$	-2.43	-1.40	-1.39
$*NH+NH_3$	-2.48	-2.39	$*NH_2NH_2$	-2.13	-2.05	-2.07
$*NH_2+NH_3$	-4.96	-2.88	$*NH_2+NH_3$	-4.96	-2.88	-2.89
$*NH_3+NH_3$	-4.83	-3.96	$*NH_3+NH_3$	-4.83	-3.96	-3.91

Table S2. B-C bond length in NRR via the alternating pathway.

Adsorbed species	$*N_2$	$*N_2H$	*NHNH	$*NH_2NH$	$*NH_2NH_2$	$*NH_2$	$*NH_3$
B-C bond length	1.49	1.51	1.50	1.53	1.50	1.54	1.50

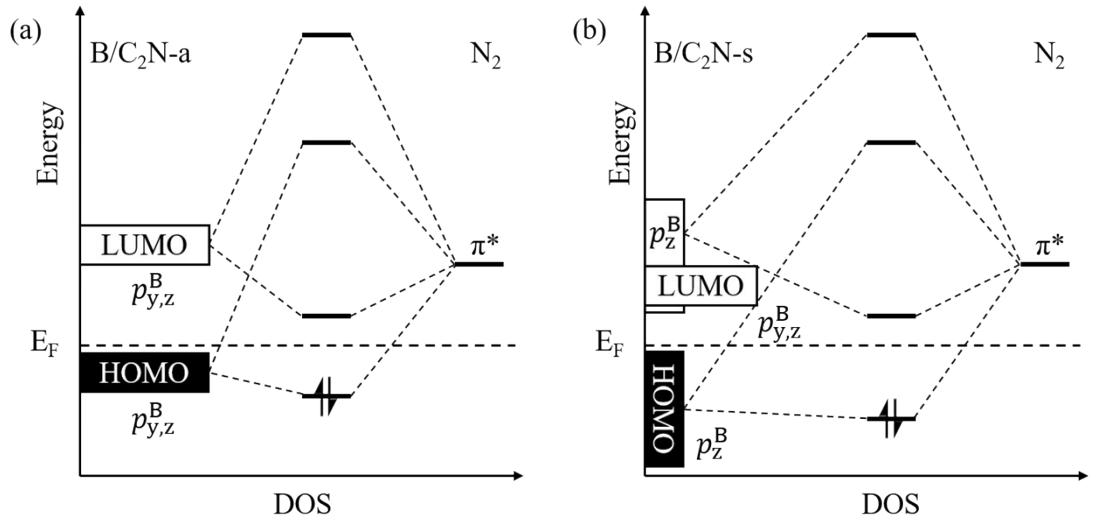

Scheme S1. Schematic diagrams of the orbital interaction for N_2 adsorption on (a) B/C_2N-a and (b) B/C_2N-s.

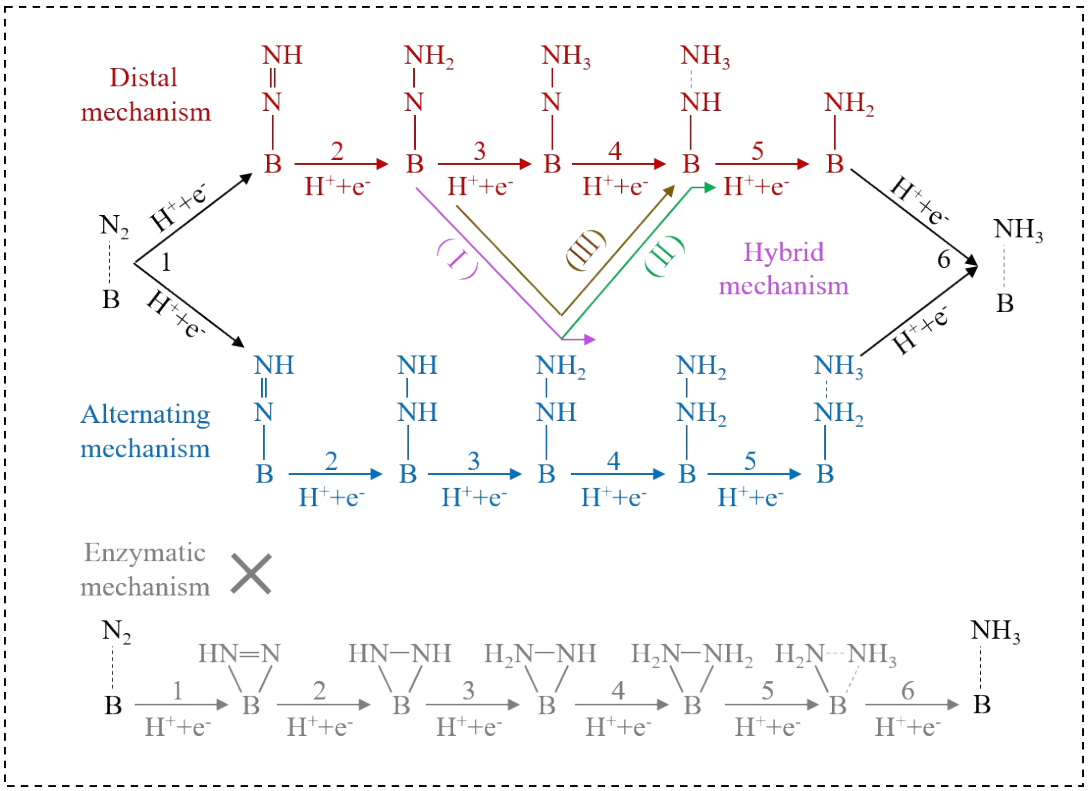

Scheme S2. Schematic illustration of possible reaction paths for N_2 reduction to NH_3.

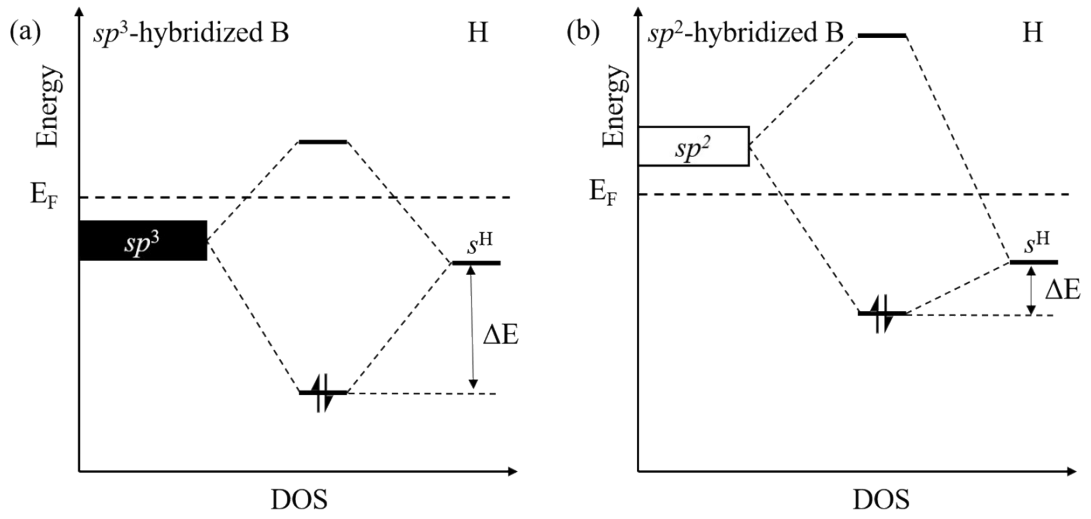

Scheme S3. Schematic diagrams of the orbital interaction for H bonding with sp^3- and sp^2-hybridized B.

$$\Delta E = \frac{|H_{ij}|^2}{E_i^0 - E_j^0} \qquad \text{Equation S1}$$

where E_i^0 is an unperturbed orbital energy before a perturbation or interaction is turned on. H_{ij} represents the matrix element of the perturbation.[3-4]

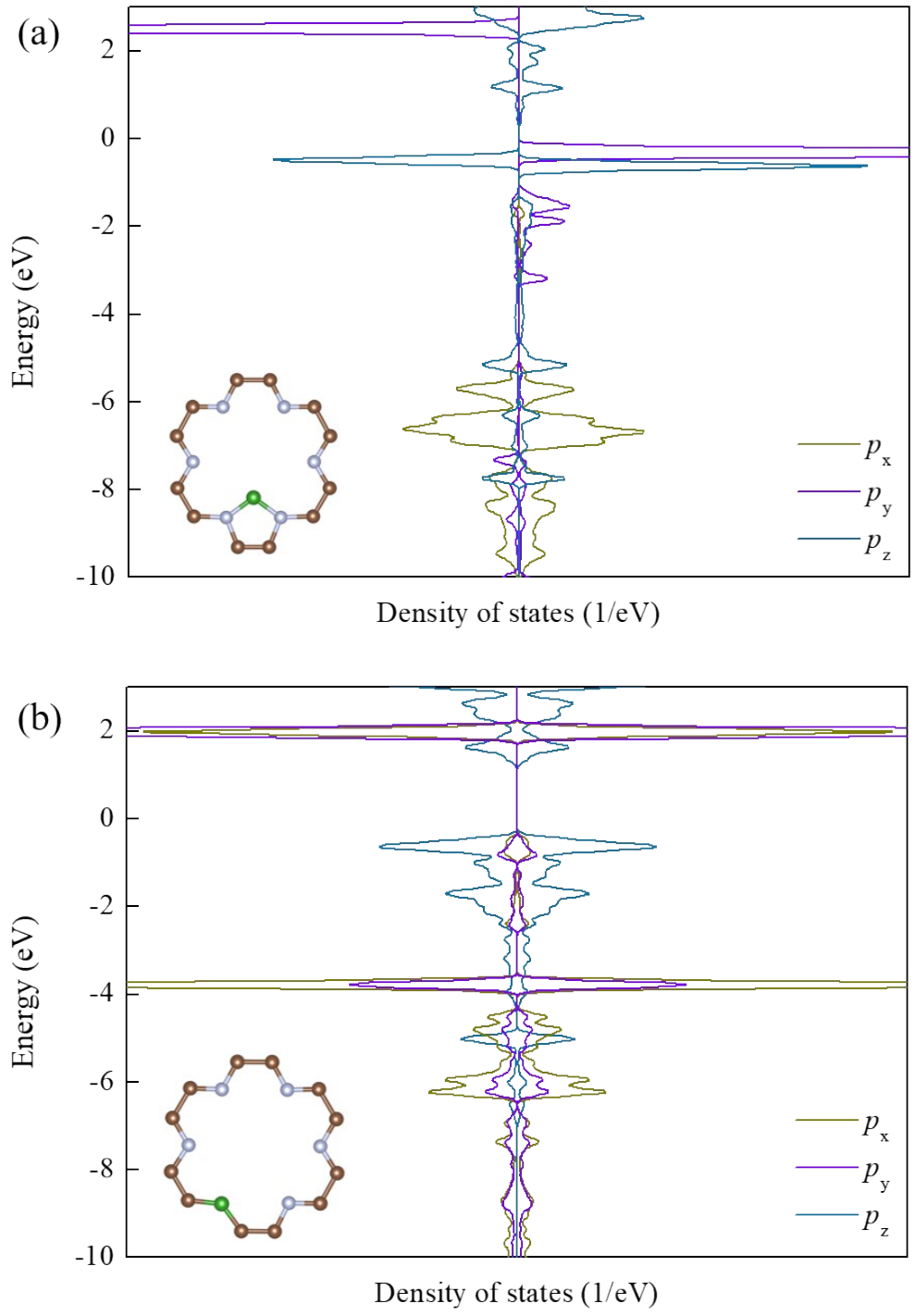

Figure S1. The pDOS of B atoms in (a) B/C_2N-a and (b) B/C_2N-s.

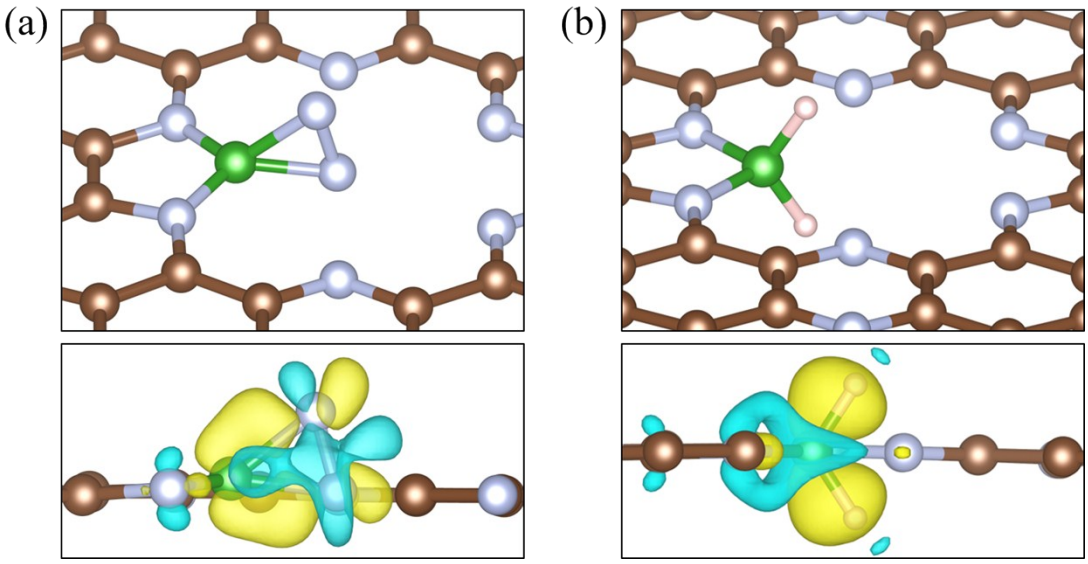

Figure S2. The geometry structure (upper panel) and differential charge densitgy (lower pannel) of (a) N_2 adsorption in side-on mode and (b) two H atoms co-adsorption on B/C_2N-a.

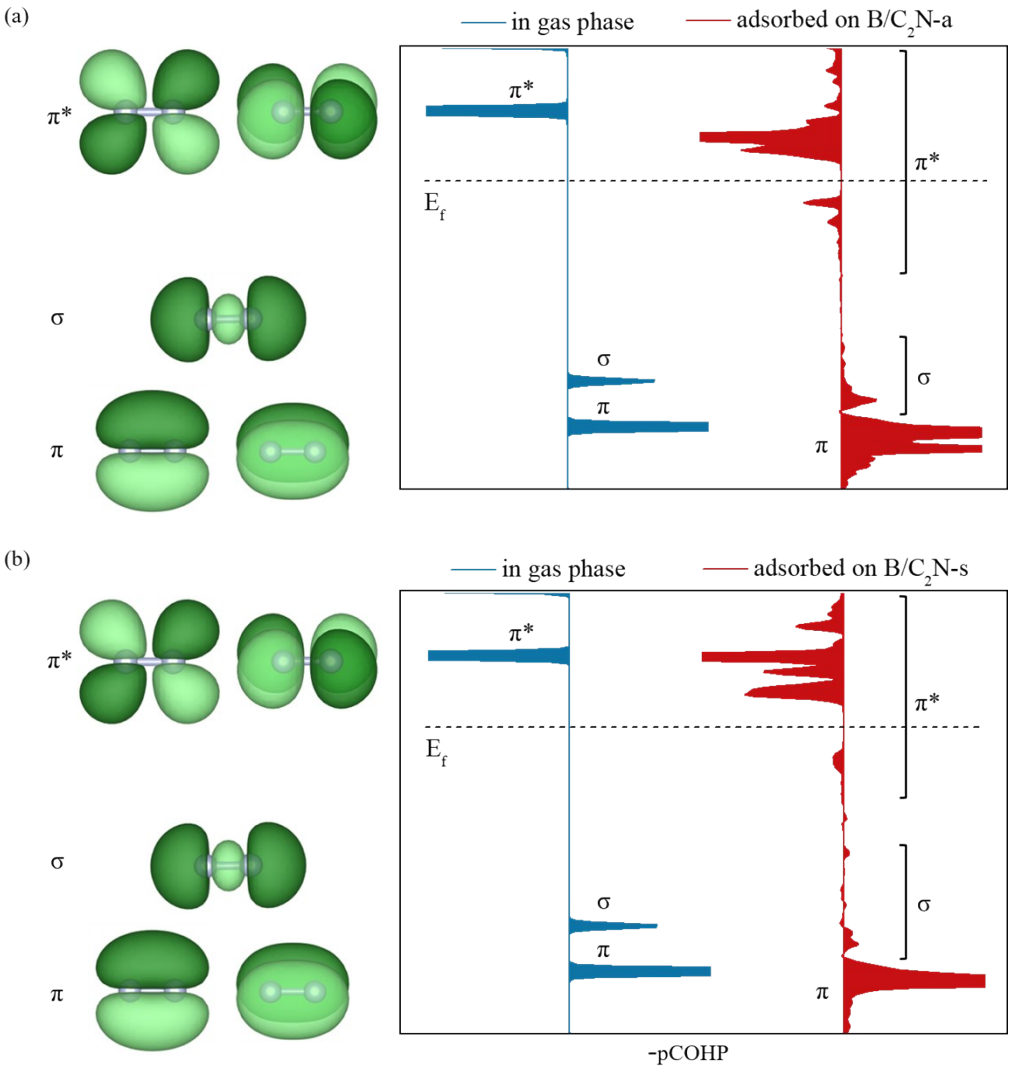

Figure S3. (a) Activation pictures of the N≡N bond after N_2 adsorption on (a) B/C_2N-a and (b) B/C_2N-s resolved by pCOHP.

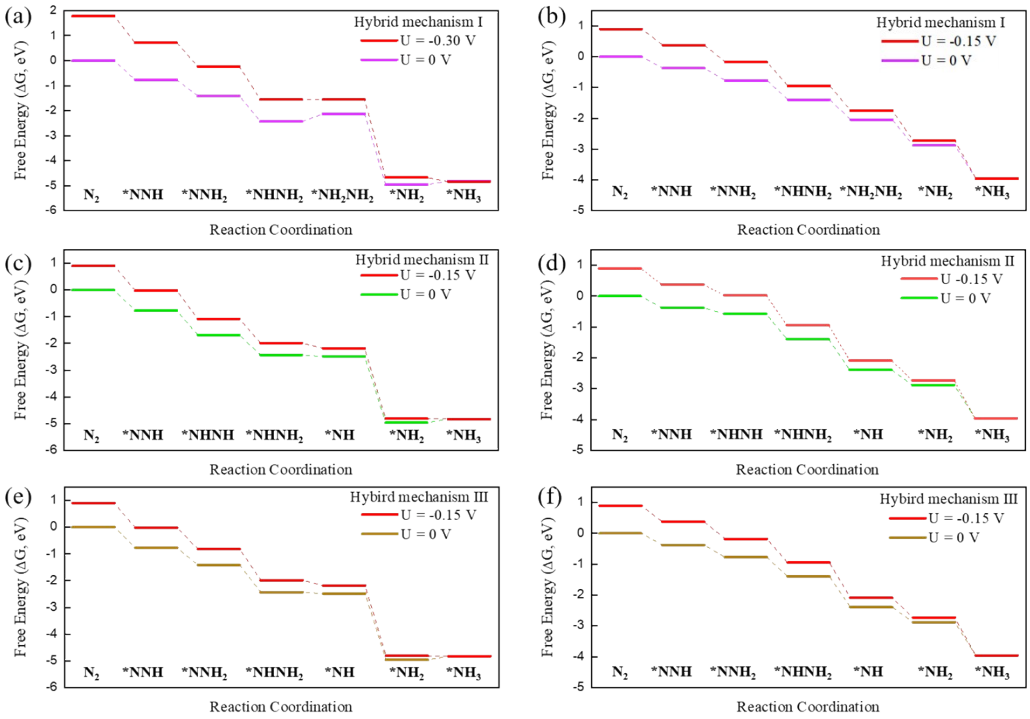

Figure S4 Free energy landscape of N_2 reduction at 0 V and the applied potential on (a, c and e) B/C_2N-a and (b, d and f) B/C_2N-s.

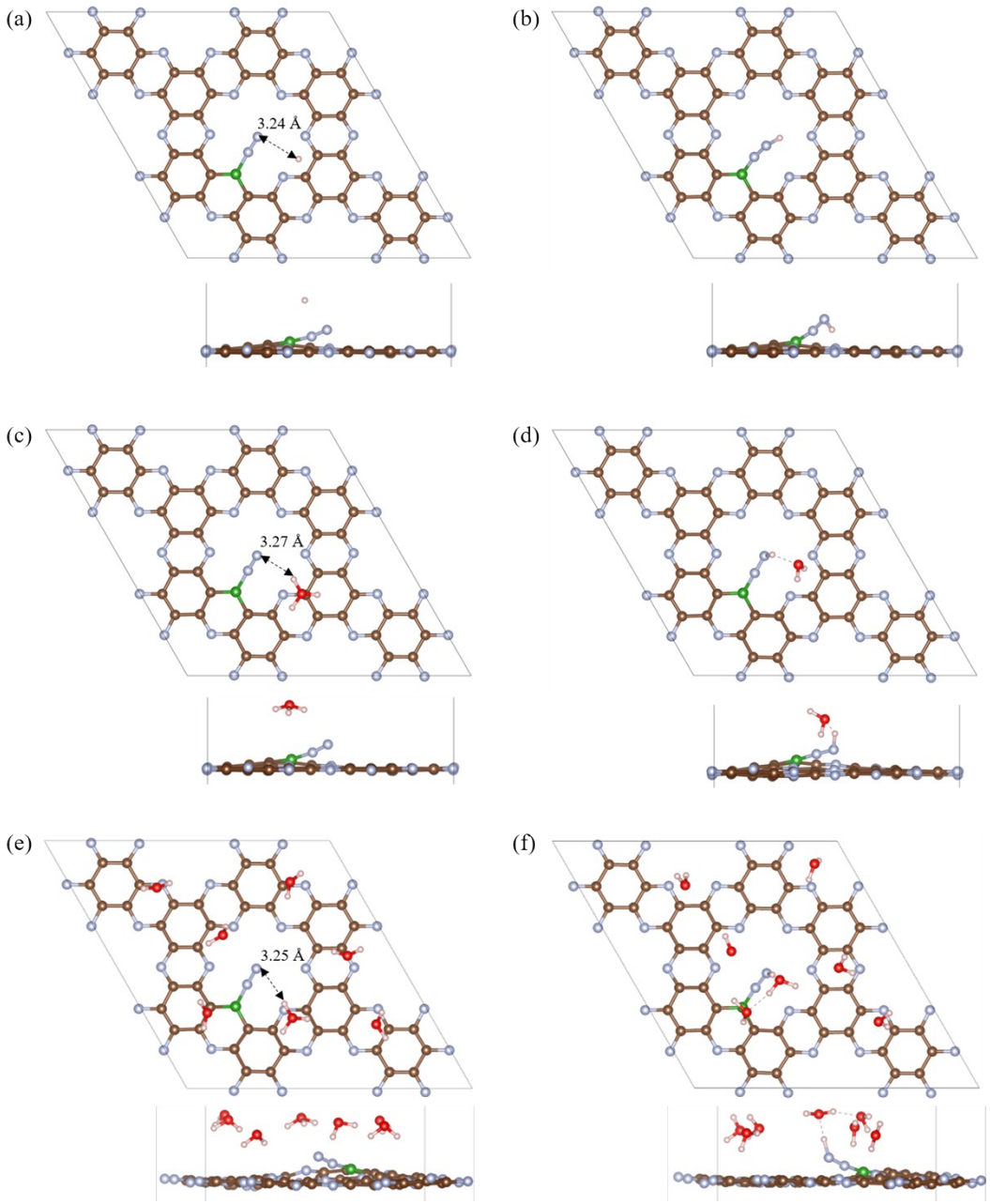

Figure S5. Initial structures of N_2 adsorption on B/C_2N-s with (a) a H atom, (c) a H_3O molecule and (e) a H_3O and several H_2O molecules in the vicinity. (b), (d) and (f) are the corresponding structure after optimization.

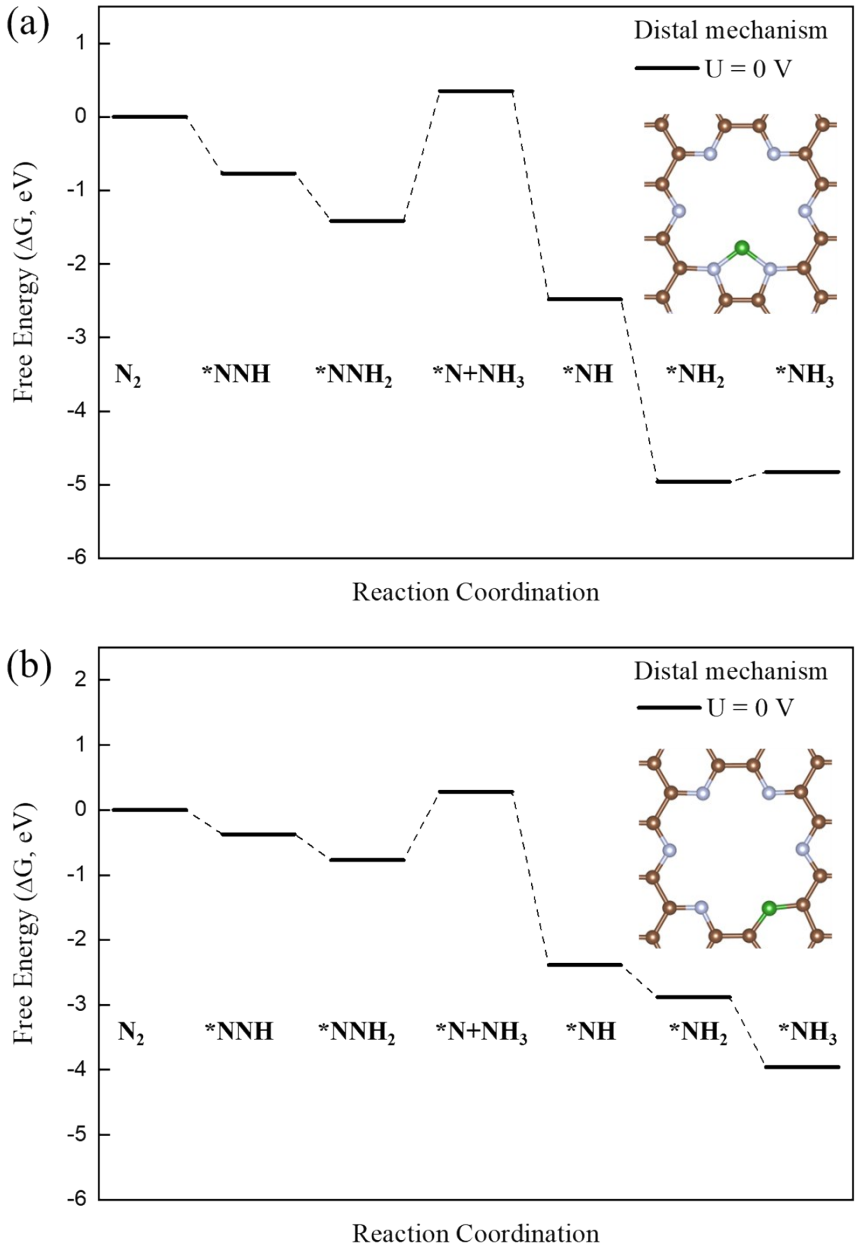

Figure S6. Free energy landscape of N_2 reduction at 0 V on (a) B/C_2N-a and (b) B/C_2N-s through distal pathway where the first NH_3 is formed by N-N bond cleavage of NNH_3.

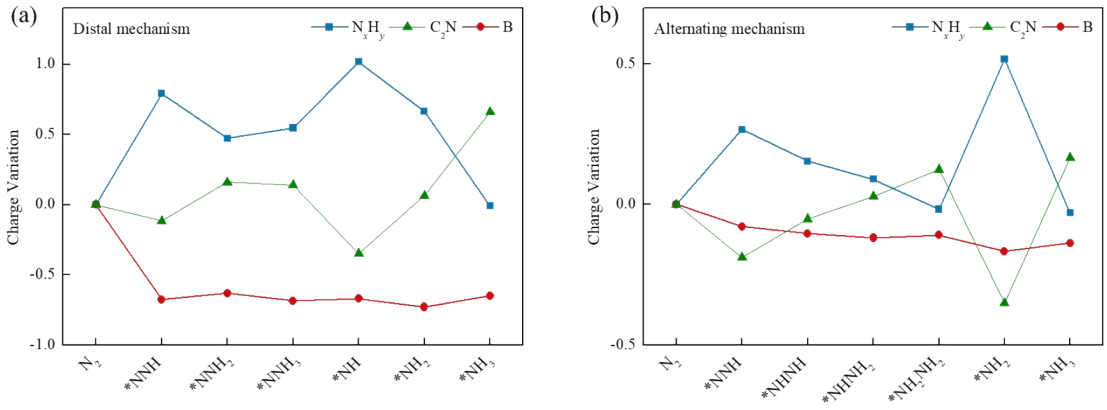

Figure S7. Bader charge of each entity in NRR process via (a) distal and (b) alternating mechanism on B/C_2N-s.

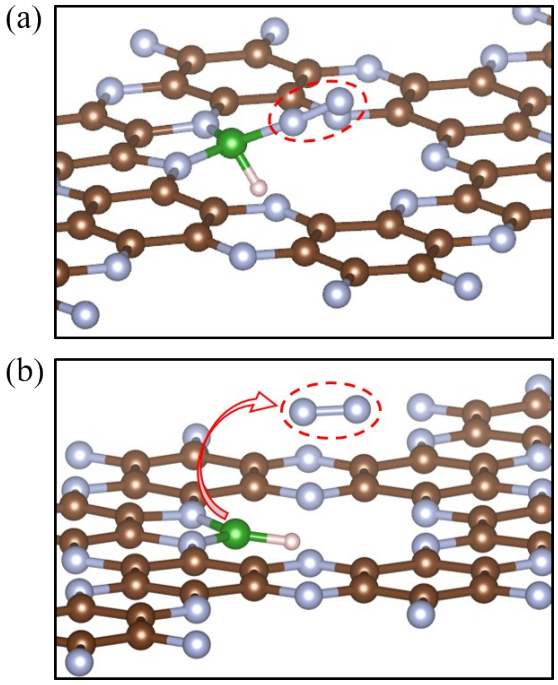

Figure S8. The geometries of N_2 and H coadsorption on B/C_2N-a (a) before and (b) after structural optimization.

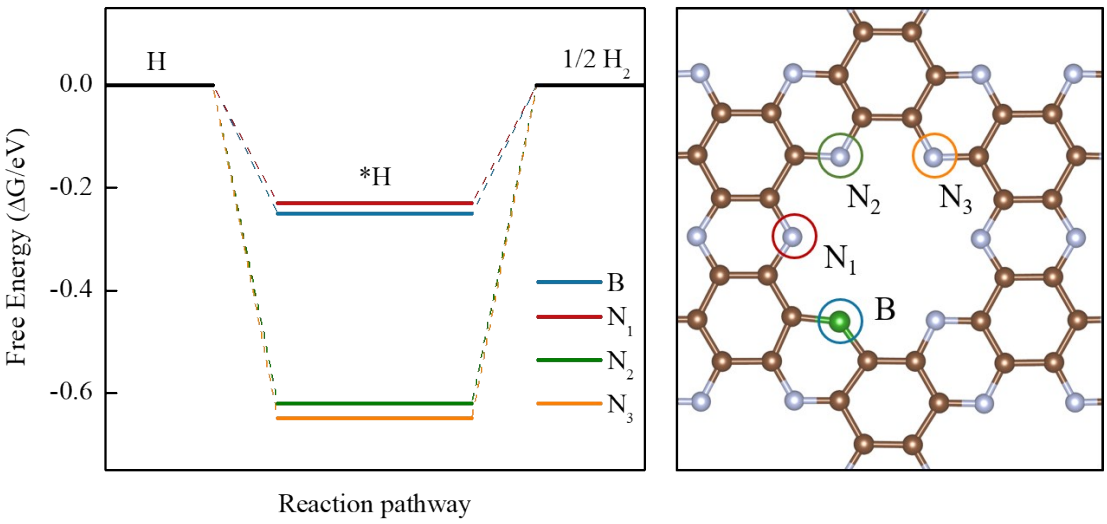

Figure S9. Free energy diagram for HER at different sites on B/C_2N-s.

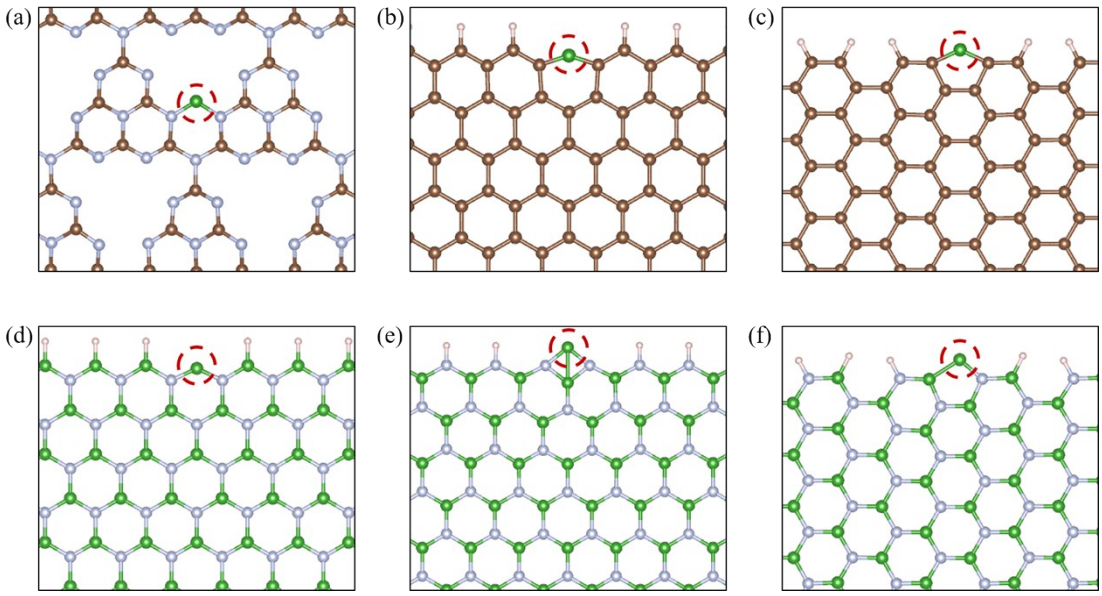

Figure S10. The optimized structures of (a) B/C_3N_4-a, (b) B/Gz-s, (c) B/Ga-a, (d) hBNz, (e) B/hBNz-a and (f) B/hBNa-a. The active B sites are marked by red circles.

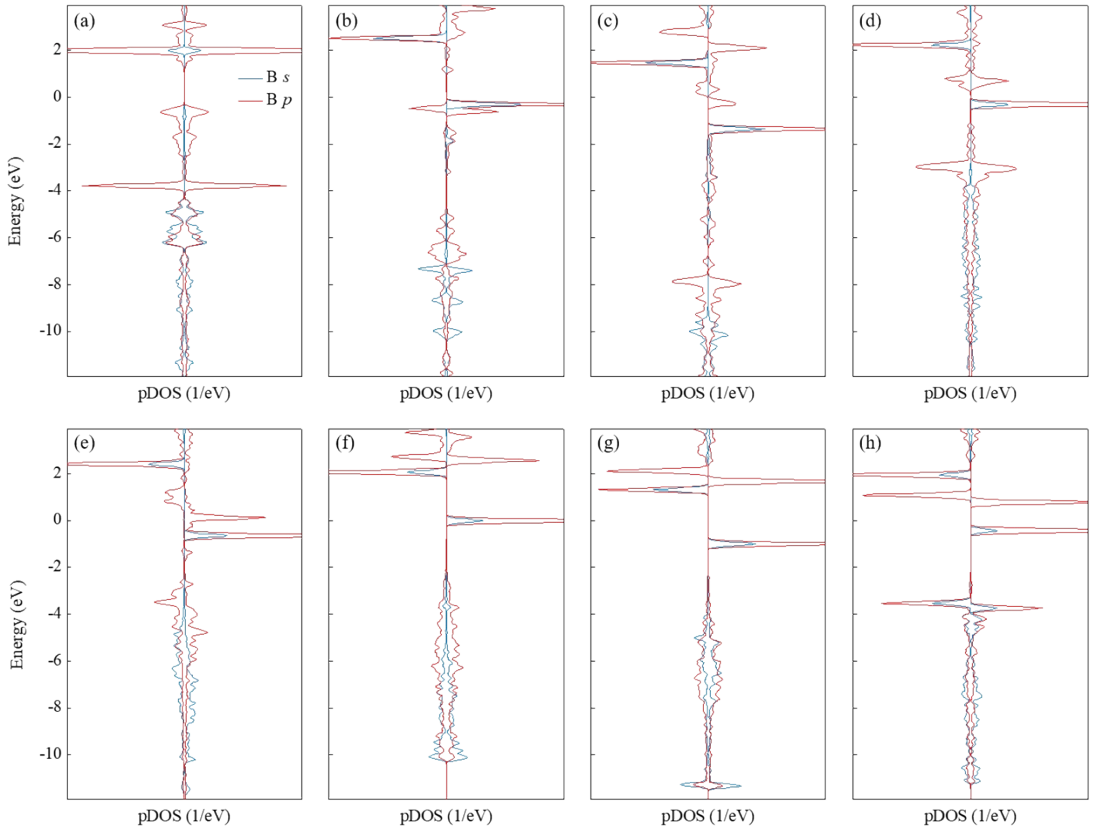

Figure S11. The pDOS of B in (a) B/C_2N-s, (b) B/C_2N-a, (c) B/C_3N_4-a, (d) B/Gz-s, (e) B/Ga-a, (f) hBNz, (g) B/hBNz-a and (h) B/hBNa-a.

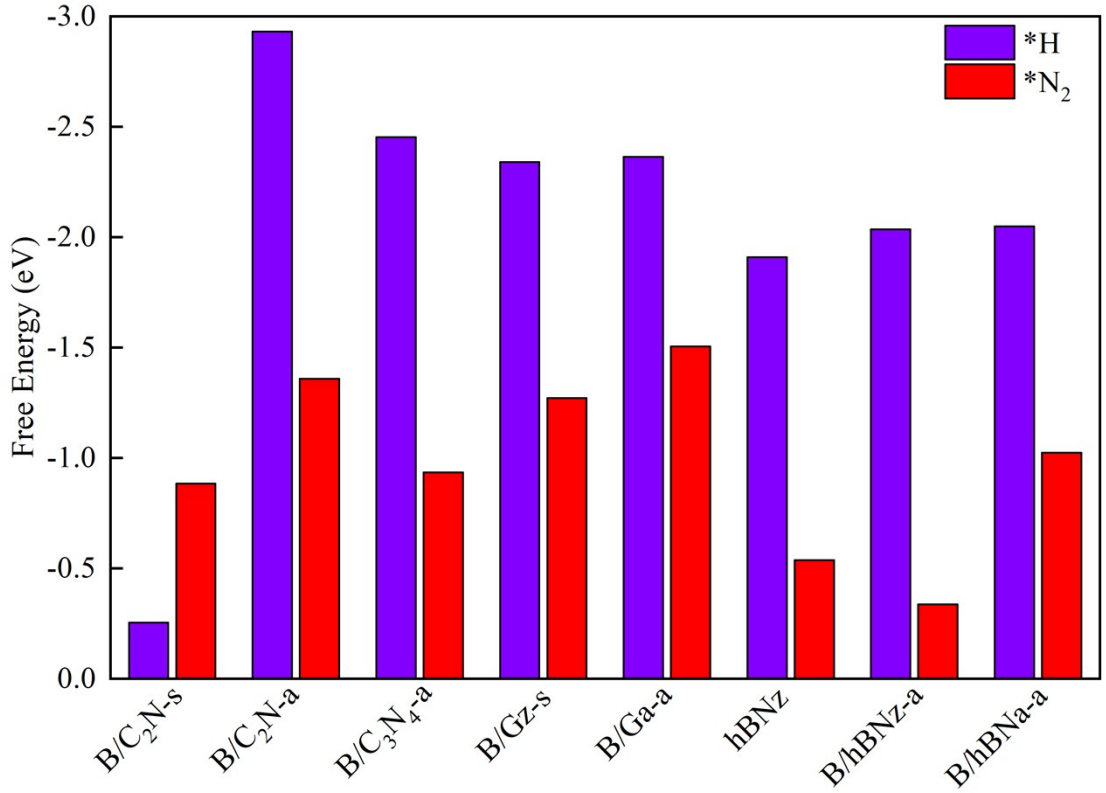

Figure S12. Free energy of H (blue) and N_2 (red) adsorption on B/C_2N-a, B/C_2N-s, B/C_3N_4-a, B/Gz-s, B/Ga-a, hBNz, B/hBNz-a and B/hBNa-a.

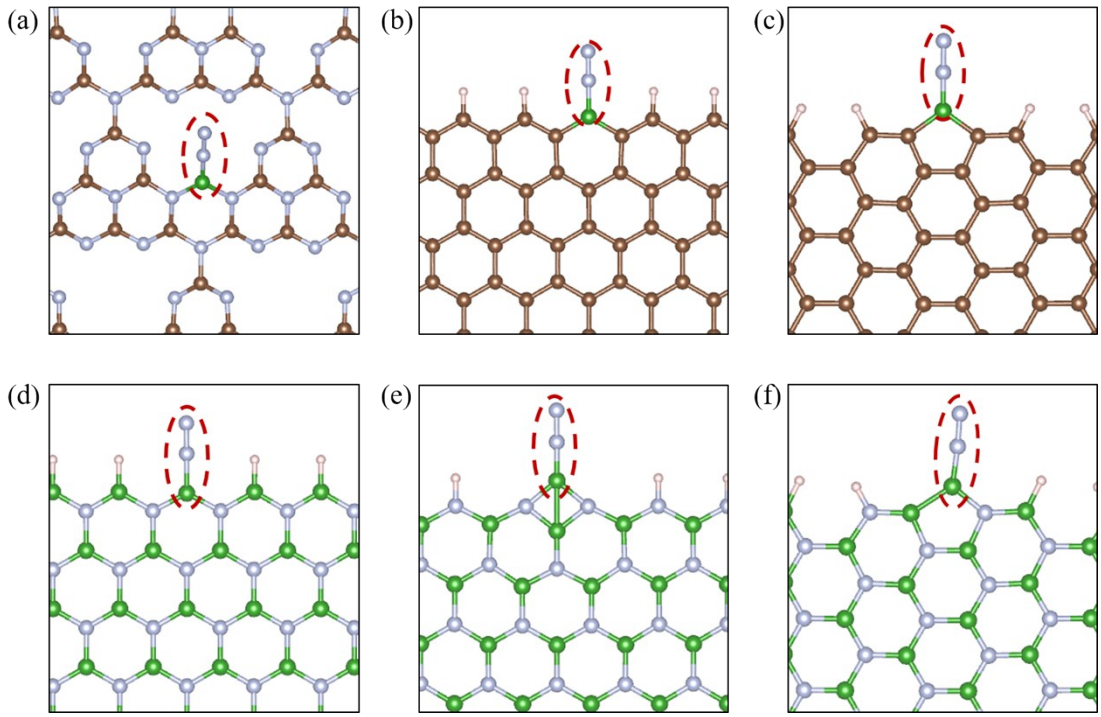

Figure S13. The optimized structures of N_2 adsorption on (a) B/C_3N_4-a, (b) B/Gz-s, (c) B/Ga-a, (d) hBNz, (e) B/hBNz-a and (f) B/hBNa-a.

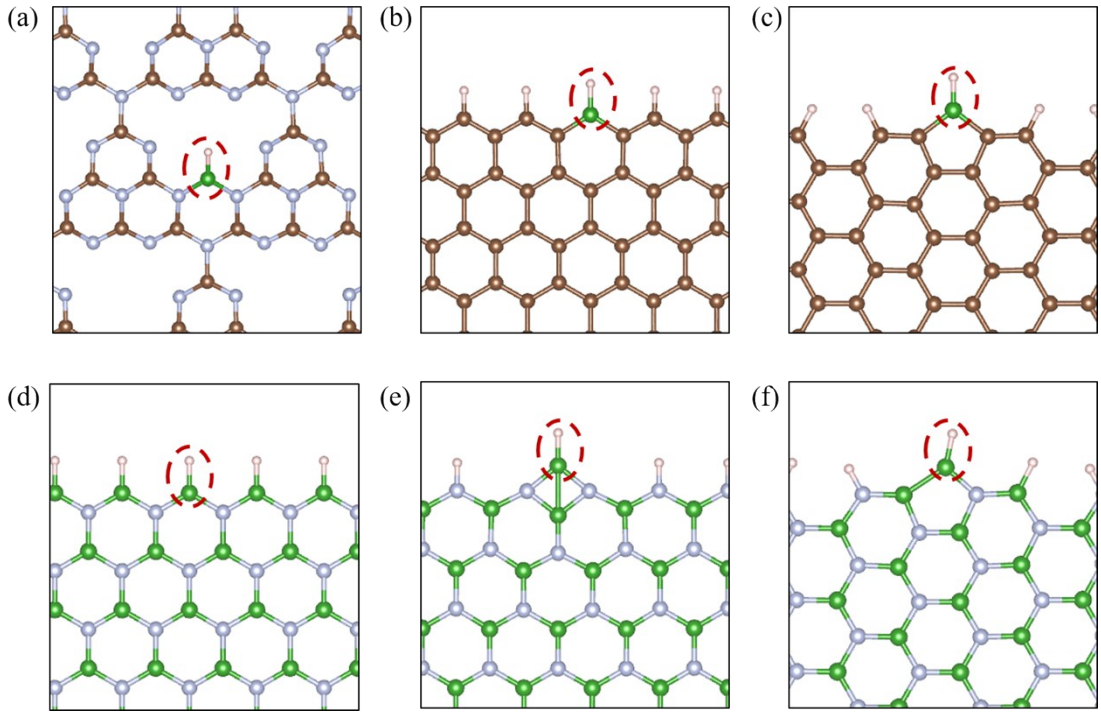

Figure S14. The optimized structure of H adsorption on (a) B/C_3N_4-a, (b) B/Gz-s, (c) B/Ga-a, (d) hBNz, (e) B/hBNz-a and (f) B/hBNa-a.

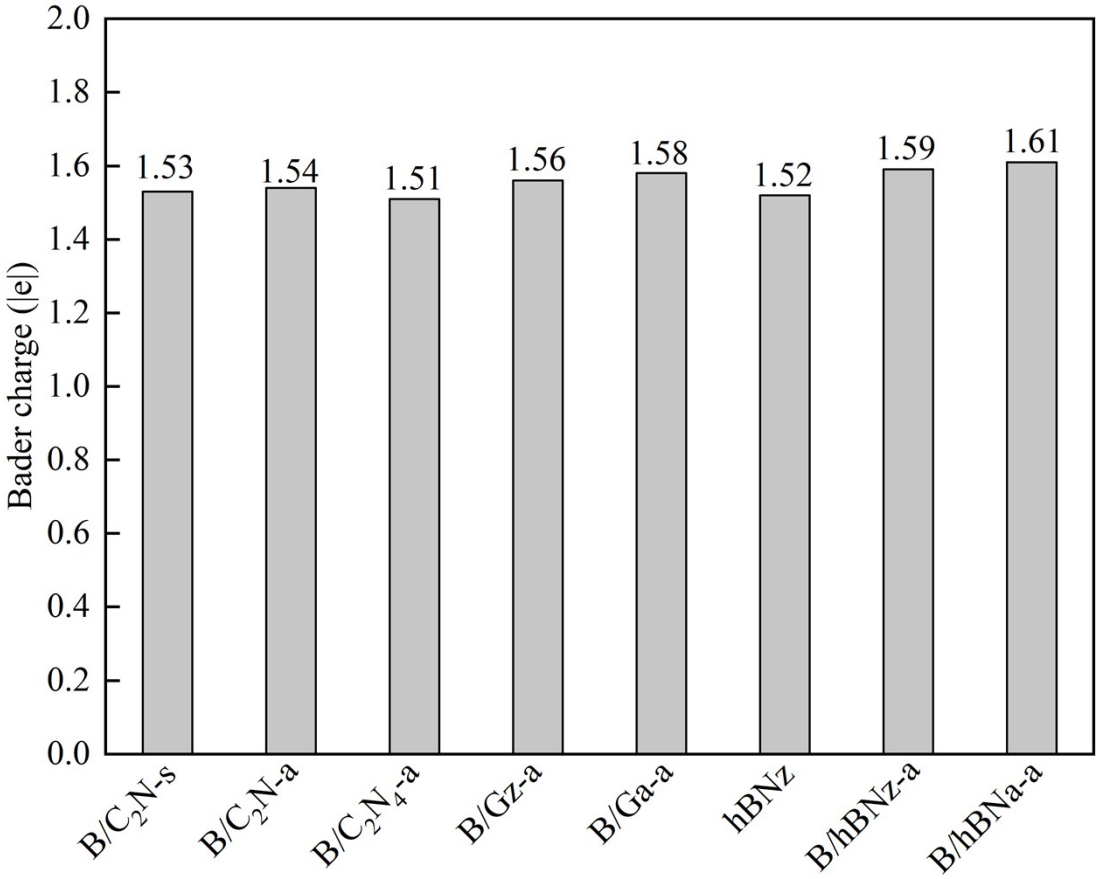

Figure S15. Bader charge of H adsorption on B/C_2N-s, B/C_2N-a, B/C_3N_4-a, B/Gz-s, B/Ga-a, hBNz, B/hBNz-a and B/hBNa-a.

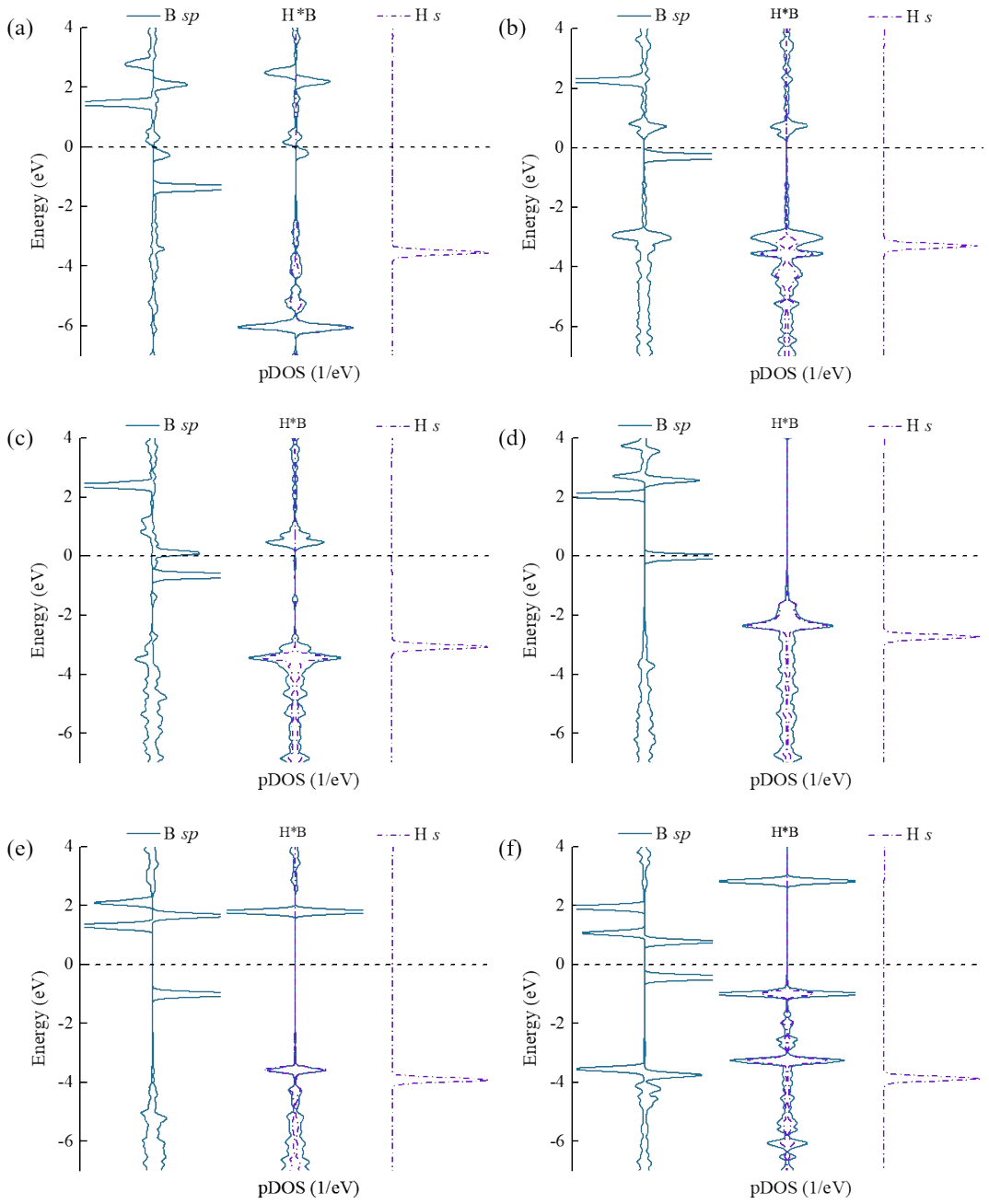

Figure S16. The pPDOS of B and H atom in (a) B/C_3N_4-a, (b) B/Gz-s, (c) B/Ga-a, (d) hBNz, (e) B/hBNz-a and (f) B/hBNa-a before and after H adsorption.

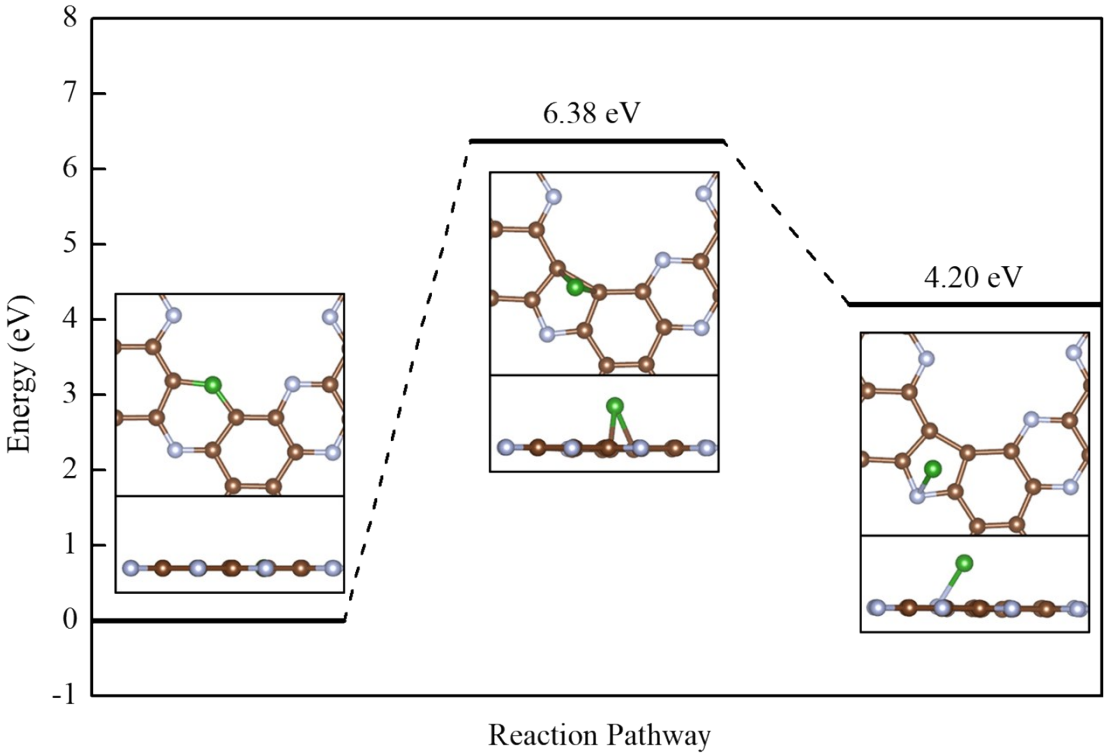

Figure S17. The minimum energy path for B hopping out of the trapping center in B/C_2N-s.

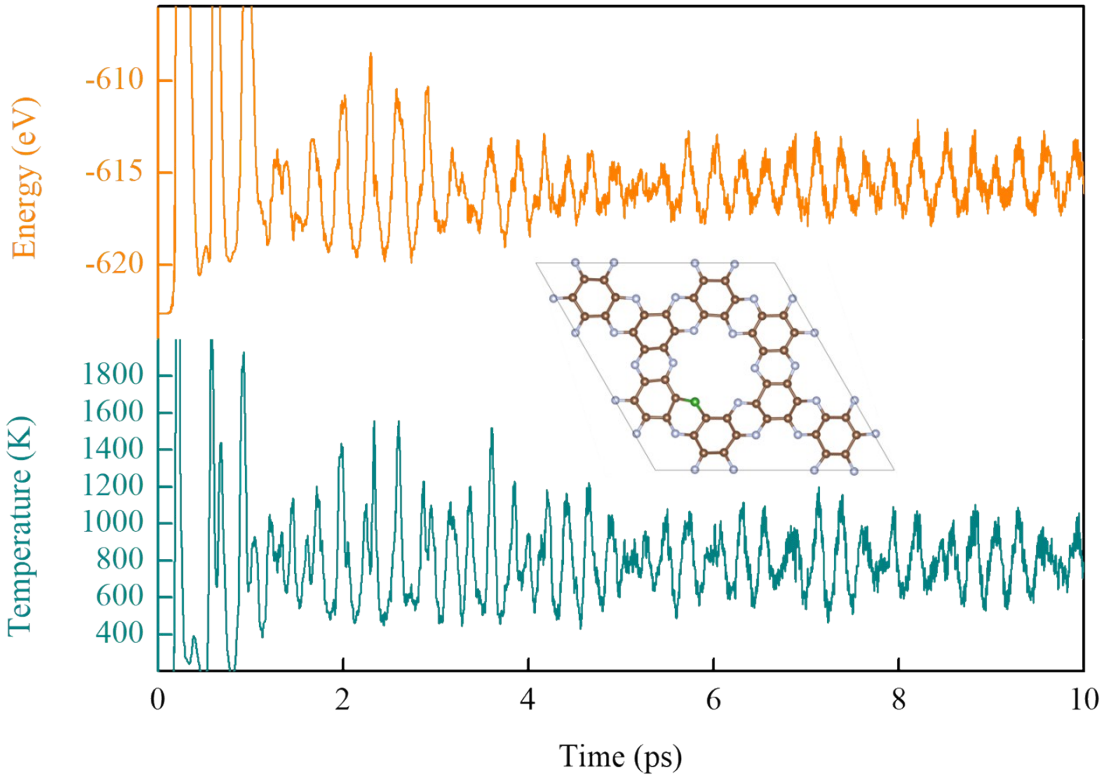

Figure S18. Variations of energy (orange) and temperature (olive) against the time in *ab initio* molecular dynamics simulations for B/C_2N-s. Insert shows the structure of B/C_2N-s after 10-ps simulation. The temperature is set to be 800 K and the time step is 2 fs.

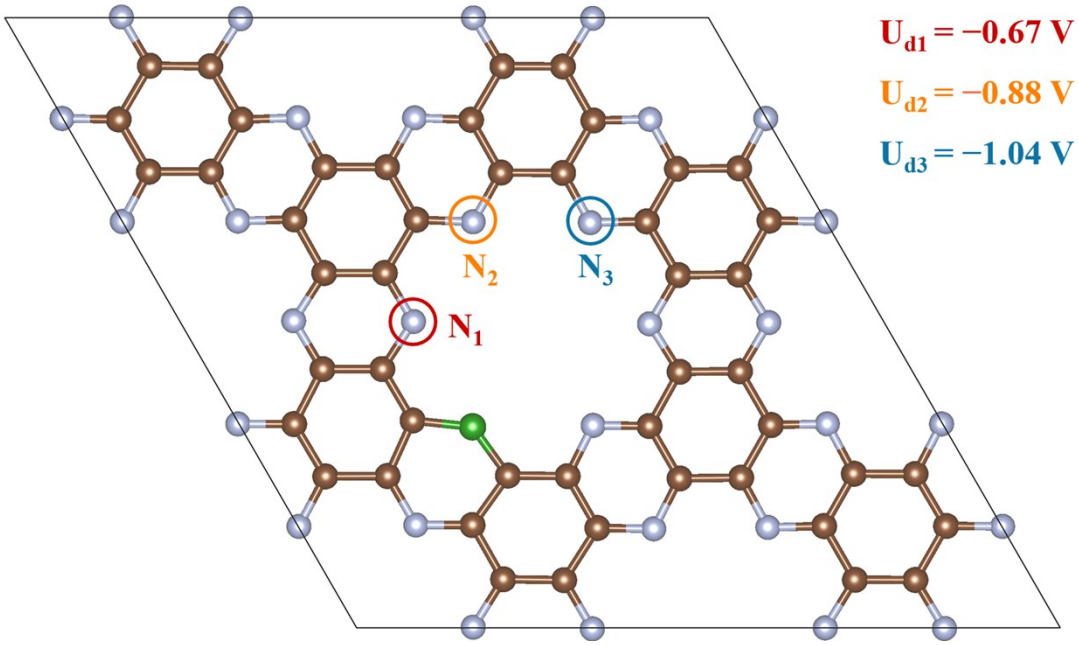

Figure S19 The decomposition potentials at three nonequivalent N sites in B/C_2N-s.

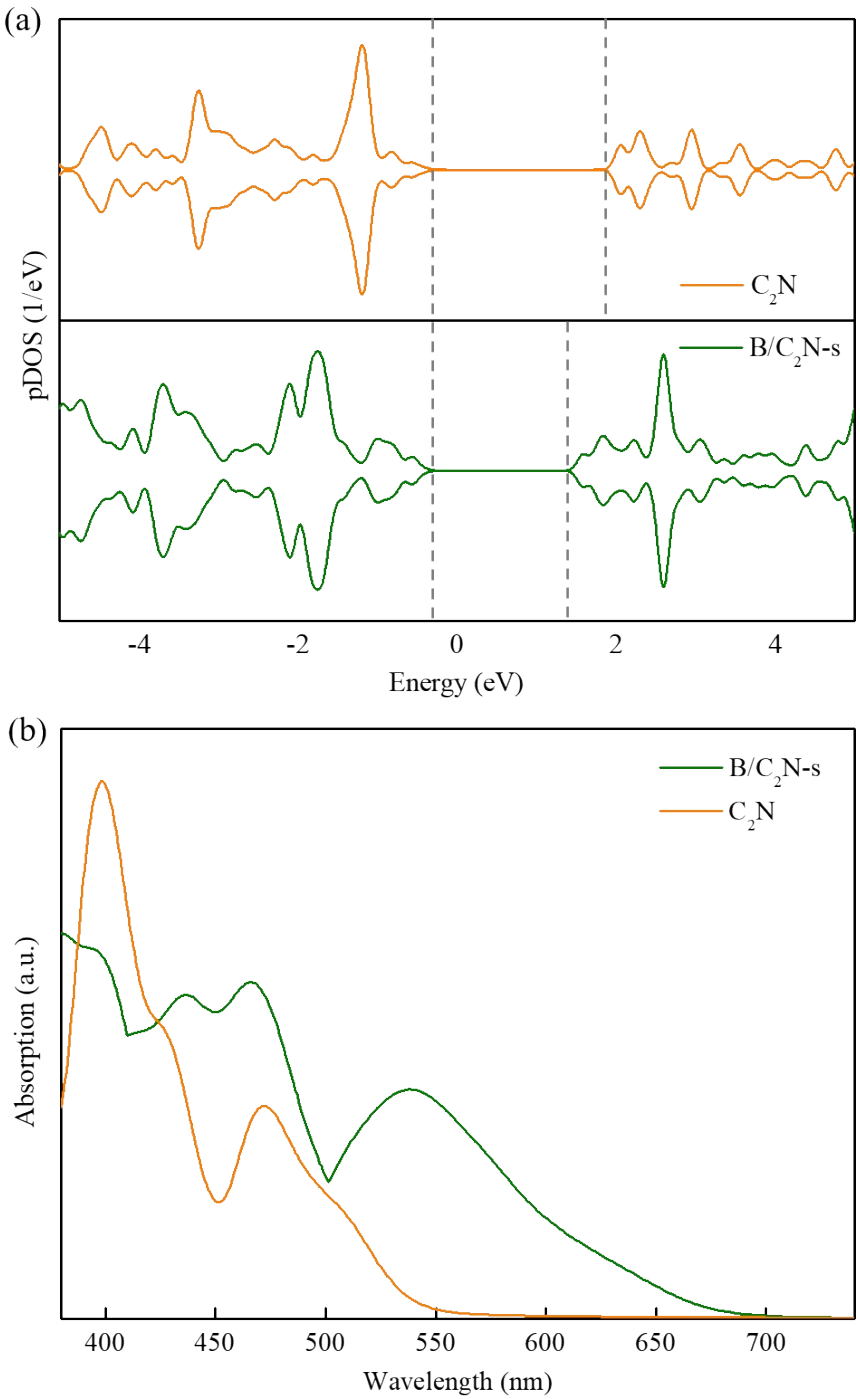

Figure S20. Comparison of (a) pDOS and (b) optical adsorption spectra for pristine C_2N and B/C_2N-s.

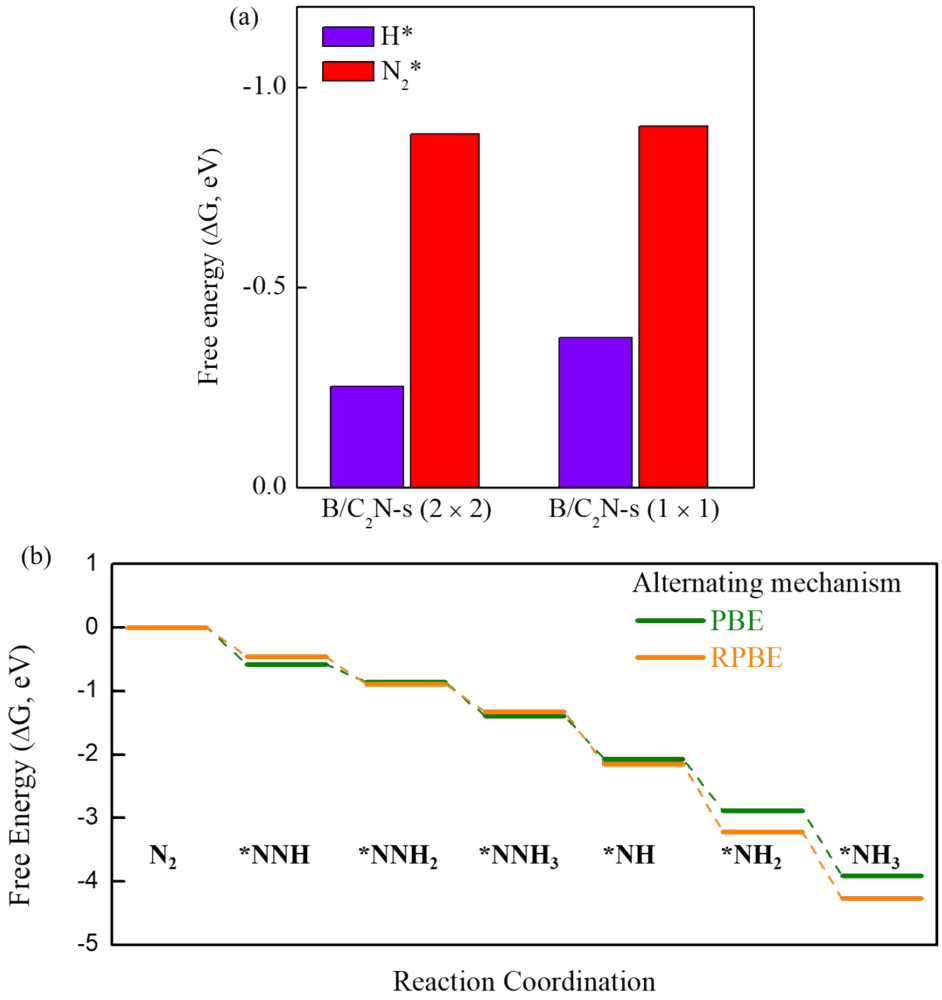

Figure S21. (a) The adsorption free energy of N_2 and H adsorption on B/C_2N-s in a 2 × 2 and 1 × 1 supercell. (b) The free energy diagram of NRR on B/C_2N-s in a 1 × 1 supercell, using Perdew-Burke-Ernzerh (PBE) and revised Perdew-Burke-Ernzerhof (RPBE) functionals, respectively.

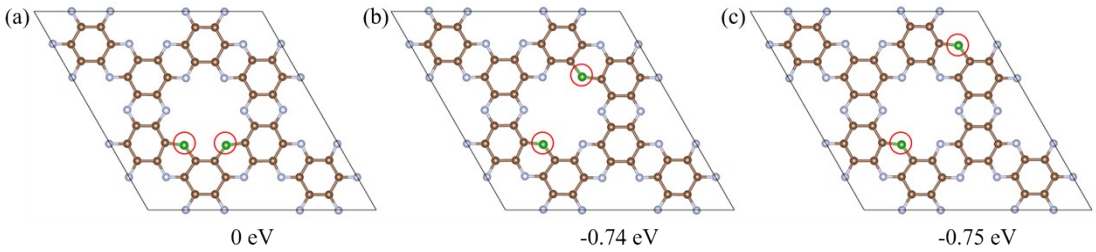

Figure S22. Relative energies of C_2N with two (a) adjcent and (b) diagonal N atoms in one cave and (c) two N atoms in two caves substituted by two B atoms.

References

(1) Skúlason, E.; Bligaard, T.; Gudmundsdottir, S.; Studt, F.; Rossmeisl, J.; Abild-Pedersen, F.; Vegge, T.; Jonsson, H.; Nørskov, J. K. A Theoretical Evaluation of Possible Transition Metal Electro-Catalysts for N_2 Reduction. *Phys. Chem. Chem. Phys.* **2012,** *14*, 1235-1245.

(2) Nørskov, J. K.; Rossmeisl, J.; Logadottir, A.; Lindqvist, L.; Kitchin, J. R.; Bligaard, T.; Jonsson, H. Origin of the Overpotential for Oxygen Reduction at a Fuel-Cell Cathode. *J. Phys. Chem. B* **2004,** *108*, 17886-17892.

(3) Albright, T. A.; Burdett, J. K.; Whangbo, M.-H., *Orbital Interactions in Chemistry*; John Wiley & Sons: 2013.

(4) Hoffman, R., *Solids and Surfaces: A Chemist's View of Bonding in Extended Structures*; VCH: Weinheim and New York, 1988.